Bone 58 (2014) 177–184

Contents lists available at ScienceDirect

Bone

journal homepage: www.elsevier.com/locate/bone

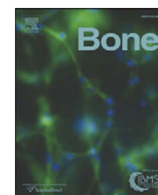

Original Full Length Article

A pre-clinical murine model of oral implant osseointegration

S. Mouraret [a,b], D.J. Hunter [a], C. Bardet [a,c], J.B. Brunski [a], P. Bouchard [b], J.A. Helms [a,*]

[a] Division of Plastic and Reconstructive Surgery, Department of Surgery, Stanford School of Medicine, Stanford, CA 94305, USA
[b] Department of Periodontology, Service of Odontology, Rothschild Hospital, AP-HP, Paris 7 Denis, Diderot University, U.F.R. of Odontology, Paris, France
[c] Dental School University Paris Descartes PRES Sorbonne Paris Cité, EA 2496 Montrouge, France

ARTICLE INFO

Article history:
Received 23 November 2012
Revised 31 May 2013
Accepted 10 July 2013
Available online 23 July 2013

Edited by: R. Baron

Keywords:
Dental
Histology
Maxilla
Oral cavity
Mice
Model

ABSTRACT

Many of our assumptions concerning oral implant osseointegration are extrapolated from experimental models studying skeletal tissue repair in long bones. This disconnect between clinical practice and experimental research hampers our understanding of bone formation around oral implants and how this process can be improved. We postulated that oral implant osseointegration would be fundamentally equivalent to implant osseointegration elsewhere in the body. Mice underwent implant placement in the edentulous ridge anterior to the first molar and peri-implant tissues were evaluated at various timepoints after surgery.

Our hypothesis was disproven; oral implant osseointegration is substantially different from osseointegration in long bones. For example, in the maxilla peri-implant pre-osteoblasts are derived from cranial neural crest whereas in the tibia peri-implant osteoblasts are derived from mesoderm. In the maxilla, new osteoid arises from periostea of the maxillary bone but in the tibia the new osteoid arises from the marrow space. Cellular and molecular analyses indicate that osteoblast activity and mineralization proceeds from the surfaces of the native bone and osteoclastic activity is responsible for extensive remodeling of the new peri-implant bone. In addition to histologic features of implant osseointegration, molecular and cellular assays conducted in a murine model provide new insights into the sequelae of implant placement and the process by which bone is generated around implants.

© 2013 The Authors. Published by Elsevier Inc. Open access under CC BY-NC-ND license.

Introduction

Oral implants are considered to be very successful prosthetic devices. They successfully replace the function of teeth and restore esthetics, and do so with a remarkably low failure/complication rate. Given these appealing characteristics, it is understandable that over the last decade the demand for oral implants has risen sharply [1]. With this precipitous increase has come a staggering array of implant modifications, all designed to improve the process of osseointegration. These modifications include adjustments in the time to loading [2], variations in surface characteristics [3], alterations in implant shape [4], and the addition of growth factors or other biological stimuli intended to "activate" the implant surface [5]. The extent to which most of these modifications actually improve implant osseointegration, however, is not known. Clearly, understanding the benefits and detriments of these changes is critically important if we want to maintain the successful profile of oral implants.

Consequently, it comes as somewhat of a surprise that the vast majority of experimental studies on oral implant osseointegration are conducted in long bones, rather than on the maxilla or mandible. The most often-quoted reasons for carrying out analyses of oral implants in long bones are their relative size and easy accessibility [6–8]. Long bones also contain a very large and pro-osteogenic marrow cavity, which facilitates rapid bone formation around an implant [9,10]. Furthermore, studies that we conducted in mice demonstrate that the marrow space is primarily responsible for generating this new peri-implant bone [6,10,11]. Using an in vivo loading device, we further demonstrated that defined forces delivered to the implant in the tibia in turn produce measurable deformations [12]. Using this information we have identified principal strains in the 10–20% range to stimulate osseointegration [13,14]. Genetic mouse models have been particularly helpful in identifying key variables that influence osseointegration; namely, we demonstrated that early excessive micromotion can cause fibrous encapsulation [15] and the elimination of mechanically sensitive cellular appendages such as primary cilia can obliterate the strain-induced bone formation [16,17].

All of these studies have been conducted in the tibia. The vast majority of implants are placed in the oral cavity [18] but in experimental models the oral cavity represents a novel, nearly unexplored, and particularly challenging microenvironment for implant osseointegration. Investigators have reported on the use of rat models to study oral implant osseointegration [19,20], some with considerable success [21]. Here, we sought to extend these findings using an animal model amenable to genetic manipulation. Our goal was to recapitulate this unique milieu of implant osseointegration in the oral cavity using a mouse model, where a vast armamentarium of genetic models and molecular

* Corresponding author. Fax: +1 650 736 4374.
E-mail address: jhelms@stanford.edu (J.A. Helms).

8756-3282 © 2013 The Authors. Published by Elsevier Inc. Open access under CC BY-NC-ND license.
http://dx.doi.org/10.1016/j.bone.2013.07.021

and cellular assays could be employed to understand and potentially improve the process of osseointegration.

Materials and methods

Animal care

All procedures followed protocols approved by the Stanford Committee on Animal Research. Wild type, male, skeletally mature (between 3 and 5 months old) CD1 mice that had an average weight of 28 g were obtained from the Jackson Laboratory (Bar Harbor, ME). Animals were housed in a temperature-controlled environment with 12-h light dark cycles and were given soft diet food (Bio Serv product #S3472) and water ad libitum. No antibiotics were given to the operated animals and there was no evidence of infection or prolonged inflammation at any of the surgical sites.

Implant surgery in the oral cavity

Twenty-three adult mice were anesthetized with an intraperitoneal injection of Ketamine (80 mg/kg) and Xylazine (16 mg/kg). The mouth was rinsed using a povidone–iodine solution for 1 min followed by a sulcular incision (Micro angled blade 10035-15, Fine Science Tools, USA) that extended from the maxillary first molar to the mid-point on the alveolar crest until behind the incisor. A full-thickness flap was elevated; a pilot hole was made to prepare the implant bed on the crest, 1.5 mm in front of the first maxillary molar using a Ø 0.3 mm pilot drill bit (Drill Bit City, Chicago, IL), and followed with a drill bit of Ø 0.45 mm. All drill holes were made using a low-speed dental engine (800 rpm). In cases where no implants were placed, the surgical site was carefully rinsed and closed using non-absorbable single interrupted sutures (Ethilon Monofilament 9-0, BV100-3, 5 in., Johnson & Johnson Medical, USA).

In cases where an implant was placed, the titanium implant (0.6 mm diameter titanium-6 aluminum-4 vanadium alloy "Retopins", NTI Kahla GmbH, Germany) was cut at length of 2 mm and was screwed down in the implant bed, maintained by a needle holder. A small portion of the implant was left exposed, approximating the height of the gingiva following with the standard procedure used for one-step oral implant placement. The flap was closed as described above. Following surgery, clinical examinations were performed and mice received subcutaneous injections of buprenorphine (0.05–0.1 mg/kg) for analgesia once a day for 3 days. Mice were sacrificed at 7, 14, 21 and 28 days post-surgery.

Implant surgery in the tibia

Adult wild-type mice were anesthetized as above; an incision was made over the right anterior-proximal tibia surface. Care was taken to preserve the periosteal surface. Holes were drilled through one cortex using a 1 mm drill bit (Drill Bit City, Chicago, IL). Implants were placed as described [12,14]. The skin was closed around the implant with non-absorbable sutures as described above, and pain management was followed as described above.

Sample preparation, processing, histology

Maxillae and tibias were harvested, the skin and outer layers of muscle were removed, and the tissues were fixed in 4% paraformaldehyde overnight at 4 °C. Samples were decalcified in a heat-controlled microwave in 19% EDTA for two weeks and after complete demineralization, the implant was gently removed from the samples. Specimens were dehydrated through an ascending ethanol series prior to paraffin embedding. Eight-micron-thick longitudinal sections were cut and collected on SuperFrost-plus slides for histology including Movat's pentachrome, aniline blue, and Picrosirius red staining.

Cellular assays

Alkaline phosphatase (ALP) activity was detected by incubation in nitro blue tetrazolium chloride (NBT; Roche), 5-bromo-4-chloro-3-indolyl phosphate (BCIP; Roche), and NTM buffer (100 mM NaCl, 100 mM Tris pH 9.5, 5 mM MgCl). Tartrate-resistant acid phosphatase (TRAP) activity was observed using a leukocyte acid phosphatase staining kit (Sigma). After its development, the slides were dehydrated in a series of ethanol and xylene and subsequently cover-slipped with Permount mounting media.

For TUNEL staining, sections were incubated in proteinase K buffer (20 μg/mL in 10 mM Tris pH 7.5), applied to a TUNEL reaction mixture (In Situ Cell Death Detection Kit, Roche), and mounted with DAPI mounting medium (Vector Laboratories). Slides were viewed under an epifluorescence microscope.

Immunohistochemistry

Tissue sections were deparaffinized following standard procedures. Endogenous peroxidase activity was quenched by 3% hydrogen peroxide for 5 min, and then washed in PBS. Slides were blocked with 5% goat serum (Vector S-1000) for 1 h at room temperature. The appropriate primary antibody was added and incubated overnight at 4 °C, then washed in PBS. Samples were incubated with appropriate biotinylated secondary antibodies (Vector BA-x) for 30 min, then washed in PBS. An avidin/biotinylated enzyme complex (Kit ABC Peroxidase Standard Vectastain PK-4000) was added and incubated for 30 min and a DAB substrate kit (Kit Vector Peroxidase substrate DAB SK-4100) was used to develop the color reaction. Antibodies used include proliferating cell nuclear antigen (PCNA, Invitrogen) Osteocalcin (Abcam ab93876), Decorin (NIH LF 113), Osteopontin (NIH LF 175), Fibromodulin (NIH LF 149), and Procollagen 1(NIH LF42). Each immunostaining reaction was accompanied by a negative control, where the primary antibody was not included.

Histomorphometric analyses

Maxillas were collected on postsurgical days 7, 14, 21, and 28 to quantify the amount of new bone generated in response to the implant. All maxilla were embedded in paraffin and sectioned longitudinally. The 0.6-mm implant was represented across ~20 tissue sections, each of which was 8 μm thick. Of those 20 sections, we used a minimum of 4 sections to quantify the amount of new bone. All the tissue sections were stained with aniline blue, which labels osteoid matrix. The sections were photographed using a Leica digital imaging system at the same magnification (×10 objective). The resulting digital images were analyzed with Adobe Photoshop CS5 software. We chose a fixed, rectangular region of interest (ROI) that in all images corresponded to 10^6 pixels. The injury site was always represented inside this ROI by manually placing the box in the correct position on each image.

The aniline blue-positive pixels were partially automated by using the magic wand tool set to a color tolerance of 60. This tolerance setting resulted in highlighted pixels with a range of blue that corresponded precisely with the histological appearance of osseous tissue in the aniline blue-stained sections. Native bone or bone fragments resulting from the drill injury were manually deselected. The total number of aniline blue-positive pixels for each section was recorded. The pixel counts from individual sections were averaged for each sample, and the differences within and among treatment groups were calculated based on these averages.

Statistical analyses

Results are presented as the mean $\pm$ SEM. Student's t-test was used to quantify differences described in this article. $P \leq 0.01$ was considered to be significant.

Download English Version:

https://daneshyari.com/en/article/5890486

Download Persian Version:

https://daneshyari.com/article/5890486

Daneshyari.com